Electronics and Communications in Japan, Part 2, Vol. 73, No. 7, 1990
Translated from Denshi Joho Tsushin Gakkai Ronbunshi, Vol. 72-CI, No. 9, September 1989, pp. 521-528

Optical Transfer Properties of Two-Photon-Pumped Image Upconverter--In the Case of Gaussian Beam Pumping

Atsushi Okamoto, Teruhito Mishima, and Ichiro Sakuraba, Members

Faculty of Engineering, Hokkaido University, Sapporo, Japan 060

SUMMARY

Spatial frequency transfer properties are analyzed for the parametric image upconverter using Gaussian beam pumping. First, the Fourier spectra of the pumping Gaussian beams on the interaction plane are derived by taking account of lateral shifts of the beams and the incident spatial frequency with respect to the upconversion system. The spatial-frequency transfer equation for thin nonlinear medium is applied to this Gaussian beam system so that the Fourier spectrum of the sum frequency optical response is derived for an infrared plane-wave input. Specifically, it is shown that the phase matching property of the image upconverter is dependent not only on the directions of the pumping beams but also on the geometric relationship between the two beams, the spot sizes and the radii of curvatures at the interaction plane.

Second, the optical field distributions of the sum frequency response for the unit-impulse infrared input is derived. From this, the relationship between the overlap of the two pumping beams and the conversion efficiency of the system is derived. Also, the imaging equations of the Gaussian beam pumping system are derived and compared with those available for the plane wave pumping and the point source pumping so that generality of the present imaging equations is confirmed.

1. Introduction

The two-photon-pumped image upconverter is a parametric four-wave mixing image device in which nonlinear optical materials such as alkaline metal vapor are used for direct conversion of an infrared image to the sum-frequency optical image. This device can make use of superior detectors in the visible region without scanning and cooling [1 - 3].

To analyze the properties of the image upconverter, we have proposed an analysis method of the image upconverter in the spatial frequency domain [4, 5]. The coupled wave equations in the spatial frequency domain have already been derived which describe the parametric interactions [5], and the analysis on the phase matching and the imaging properties for the plane wave pumping system has been carried out [6, 7]. It was confirmed that these results are not contradictory to the conventional analysis in the space domain [8, 9]. However, if the output from the laser or the optical parametric oscillator is used for pumping, it is necessary to assume a Gaussian beam pumping.

Although this situation is of practical importance, no sufficient studies have been carried out. Also, since it is difficult to handle this system with a conventional geometric optics method, an analysis in the spatial frequency domain has been desired.

In this paper, the spatial frequency transfer properties are analyzed for the parametric image upconverter using a Gaussian beam pumping, and the phase matching and the imaging properties are reported for the first time.

First, the Fourier spectra of the pumping Gaussian beams on the interaction plane are derived by taking into consideration the lateral shift of the beams (in the space domain) for the upconversion system and the lateral shift of the spectra in the spatial frequency domain. The results are applied

ISSN8756-663X/90/0007-0023$7.50/0

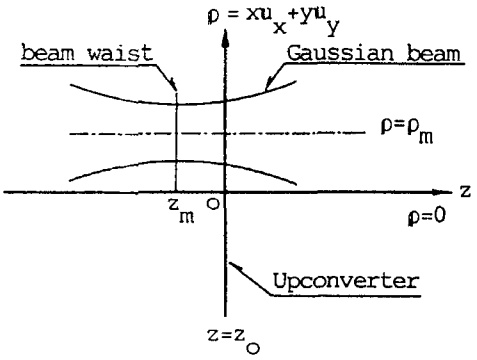

Fig. 1. Coordinate system of collinear Gaussian beam.

to the spatial frequency transfer equation of an infinitesimally thin medium so that the transfer equation between the input and the output images is derived for the Gaussian beam pumping.

Second, the sum frequency response of the upconversion system is derived for the infrared plane wave input so that the phase matching characteristics of the system are discussed in the spatial frequency domain.

Further, by deriving the sum-frequency optical field distribution for the infrared unit impulse field, the imaging equations are derived for the Gaussian pumping system. The results are compared with those for the point source and the plane-wave pumping systems.

In the following analysis, it is assumed for simplicity that the nonlinear medium is sufficiently thin and all the optical waves are paraxial rays. In general, the upconverter using a two-photon-pumped medium can realize a significantly larger conversion efficiency than the conventional ones using a nonlinear optical crystal [1]. However, when it is used as an image upconverter, the quantum efficiency is reduced to several percent as the spot sizes of the pumping beams are increased and the medium is made thin so that the image quality is improved [10]. Hence, the attenuations of the infrared and pumping waves due to the nonlinear interaction effect are sufficiently small so that the envelopes of these optical waves can be taken as a constant in the nonlinear medium.

It is assumed that the aperture of the medium is much larger than both spot sizes of the Gaussian beams. It is also assumed that the diffraction effect by the medium aperture is negligible. It is assumed further that the refraction index of the nonlinear medium is equal to unity and the wavelengths of the optical waves in the medium are equal to those in vacuum.

2. Fourier Spectrum of the Gaussian Beam

In the coordinate system shown in Fig. 1, the optical axis of the upconverter is taken along the z axis and the transverse spatial coordinate (x, y) is given by

$$\boldsymbol{\rho} = x\boldsymbol{u}_x + y\boldsymbol{u}_y \tag{1}$$

where $\boldsymbol{u}_x$ and $\boldsymbol{u}_y$ are the unit vectors in the x and y directions.

If the two pumping beams are distinguished by the subscripts $m = 1, 2$, the Gaussian beam of the fundamental mode on the interaction plane ($z = z_0$) is [11]

$$E_m(\boldsymbol{\rho}\,;\, z_o) = \frac{w_{om}}{w_m}\exp\{-j(k_m z_{om} - \phi_m) - \alpha_m(\boldsymbol{\rho}-\boldsymbol{\rho}_m)^2\} \tag{2}$$

where $\boldsymbol{\rho}_m$ is the lateral shift of the Gaussian beam axis with respect to the optical axis of the upconversion system. The distance between the beam waist and the interaction plane with the nonlinear medium (lateral shift amount) is given by

$$z_{om} = z_o - z_m \tag{3}$$

Also, the parameters of the Gaussian beam are designated as

$$\alpha_m = \frac{1}{w_m^2} + \frac{jk_m}{2R_m} \tag{4}$$

$$w_m^2 = w_{om}^2\left\{1+\left(\frac{\lambda_m z_{om}}{\pi w_{om}^2}\right)^2\right\} \tag{5}$$

$$R_m = z_{om}\left\{1+\left(\frac{\pi w_{om}^2}{\lambda_m z_{om}}\right)^2\right\} \tag{6}$$

$$\phi_m = \tan^{-1}\left(\frac{\lambda_m z_{om}}{\pi w_{om}^2}\right) \tag{7}$$

where w_m is the beam spot size on the interaction plane, R_m is the radius of curvature, and w_{om} is the eigenvalue spot size. Also, k_m and λ_m are the wavenumber and the wavelength of the pumping beam in the medium.

The Fourier spectrum [5] in Eq. (2) is

$$\underline{F}_m(\boldsymbol{f}\,;\, z_o) \equiv \int E_m(\boldsymbol{\rho}\,;\, z_o)\exp\{j2\pi\boldsymbol{f}\cdot\boldsymbol{\rho}\}d^2\boldsymbol{\rho}$$

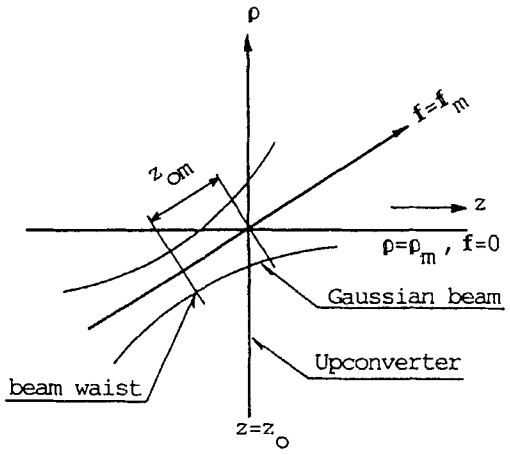

Fig. 2. Coordinate system of noncollinear Gaussian beam.

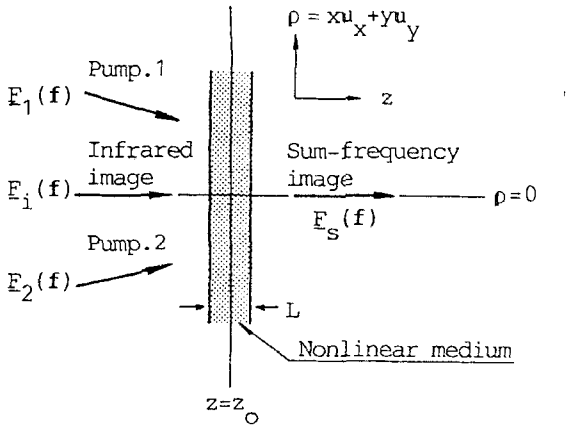

Fig. 3. Image upconverter.

$$= \frac{w_{om}}{w_m}\frac{\pi}{\alpha_m}\exp\{-j(k_m z_{om}-\phi_m)\}$$

$$\cdot\exp\left\{-\frac{\pi^2}{\alpha_m}f^2+j2\pi\rho_m\cdot f\right\} \tag{8}$$

where f is the spatial frequency (vector) for the transverse spatial coordinate ρ.

If the spectrum is parallel shifted so that the center spatial frequency of the Gaussian beam is f_m in Eq. (8),

$$\underline{F}_m(f\,;z_o)=\frac{w_{om}}{w_m}\frac{\pi}{\alpha_m}\exp\{-j(k_m z_{om}-\phi_m)\}$$

$$\cdot\exp\left\{-\frac{\pi^2}{\alpha_m}(f-f_m)^2+j2\pi\rho_m\right.$$

$$\left.\cdot(f-f_m)\right\} \tag{9}$$

As shown in Fig. 2, this corresponds to representing the inclination of the Gaussian beam with respect to the optical axis of the upconversion system in terms of the spatial frequency f_m of the wavefront at the beam waist [12]. However, this correspondence is valid only if the inclination of the Gaussian beam is small enough so that the paraxial approximation is satisfied. In the following, Eq. (9) is used as the Fourier spectrum of the Gaussian beam.

3. Spatial Frequency Transfer Equation

In the image upconverter shown in Fig. 3, the equation (the so-called spatial frequency transfer equation) is derived here for the relationship between the Fourier spectrum of the infrared wave incident to the front surface of the nonlinear medium pumped by Gaussian beams and that of the sum frequency wave emerging from the back surface. In general, a system using a two-photon-pumped medium can realize a much larger conversion efficiency than a system using a conventional nonlinear optical crystal [1]. Especially, if the upconverter is used for the sole purpose of obtained a short wavelength signal, a quantum conversion efficiency as large as several tens percent is obtained since the resolution of the upconverter is not concerned [13]. However, this result is accomplished with pumping beams with small spot sizes and a sufficiently thick nonlinear medium. If an image upconversion with a high resolution is attempted with an upconverter, it is necessary to make the spot sizes of the pumping beams large and the medium thin so that the diffraction by a finite aperture in the interaction region and the aberration due to the thickness of the nonlinear medium (thickness aberration) [8] can be avoided.

If these factors are taken into account, the quantum conversion efficiency of the presently known image upconverter using alkaline metal vapor is expected to be 1 to several percent. As an example, in the experiment by Newton et al., the quantum conversion efficiency of about 5 percent was attained with an aperture diameter of 2 cm for the image upconversion metal vapor cell (at an infrared wavelength of 2.94 μm and a pumping beam intensity of 275 kW/cm^2). Hence, in this paper, a system with a low conversion efficiency made of a sufficiently thin medium is assumed. In this case, the attenuation effects of the infrared and

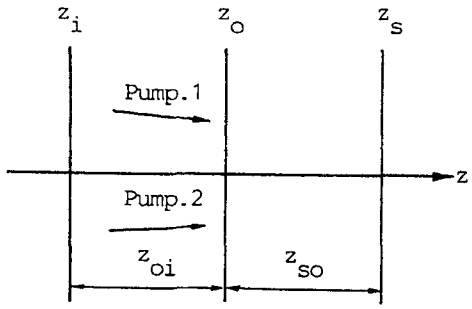

Fig. 4. Schematic diagram of image upconverter.

pumping waves are neglected as the parametric interaction is sufficiently weak. It is also assumed that the medium aperture is sufficiently larger than the spot sizes of the Guassian beams.

3.1. Spatial frequency transfer equation in a nonlinear medium

In a nonlinear medium, a sum frequency wave is generated from the incident infrared wave and the two pumping beams by the four-wave parametric interaction. In the image upconverter (in Fig. 3), the spatial frequency transfer equation between the Fourier spectra of the incident infrared wave and the output sum frequency wave is given by [7]

$$\underline{F}_s(f\ ;\ z_o)=-j\beta_s L\cdot\underline{F}_{we}(f\ ;\ z_o)*\underline{F}_i(f\ ;\ z_o) \tag{10}$$

where β_s is the coupling coefficient of the parametric interaction and L is the medium thickness. The operator * indicates the two-dimensional convolution with respect to the spatial frequency f and the subscripts i and s indicate the infrared and sum frequency waves. Also, the function $\underline{F}_{we}(f\ ;\ z_o)$ represents the diffraction effect of the incident infrared image on the interaction plane and is called here, the Fourier spectrum of the effective window function. If a situation is assumed in which the effect of the medium aperture can be neglected, the following equation is satisfied by the Fourier spectra $\underline{F}_1(f\ ;\ z_o)$ and $\underline{F}_2(f\ ;\ z_o)$ of the pumping beams [7]:

$$\underline{F}_{we}(f\ ;\ z_o)=\underline{F}_1(f\ ;\ z_o)*\underline{F}_2(f\ ;\ z_o) \tag{11}$$

3.2. Spatial frequency transfer equation between the input and output image planes

In the image upconverter shown in Fig. 4, let z_i be the location of the infrared image (input) to be converted and z_s be that of the sum-frequency optical image (output) obtained by the parametric image upconversion. If the distances between each image and the interaction plane are given by

$$\left.\begin{aligned} z_{oi}&=z_o-z_i\\ z_{so}&=z_s-z_o \end{aligned}\right\} \tag{12}$$

then the propagation of the Fourier spectrum from each image plane to the interaction plane is given by [7]

$$\underline{F}_i(f\ ;\ z_o)=\underline{F}_i(f\ ;\ z_i)\exp\left\{-jk_i z_{oi}\left[1-\left(2\pi\frac{f}{k_i}\right)^2\right]^{\frac{1}{2}}\right\} \tag{13}$$

and

$$\underline{F}_s(f\ ;\ z_s)=\underline{F}_s(f\ ;\ z_o)\exp\left\{-jk_s z_{so}\left[1-\left(2\pi\frac{f}{k_s}\right)^2\right]^{\frac{1}{2}}\right\} \tag{14}$$

where k_i and k_s are the wavenumbers of the infrared and the sum frequency waves. When Eqs. (13) and (14) are substituted into Eq. (10), the spatial frequency transfer equation between the input and output image planes is obtained:

$$\begin{aligned}\underline{F}_s(f\ ;\ z_s)=-j\beta_s L\cdot\exp&\left\{-jk_s z_{so}\left[1-\left(2\pi\frac{f}{k_s}\right)^2\right]^{\frac{1}{2}}\right\}\cdot\underline{F}_{we}(f\ ;\ z_o)\\ &*\left[\underline{F}_i(f\ ;\ z_i)\cdot\exp\left\{-jk_i z_{oi}\left[1-\left(2\pi\frac{f}{k_i}\right)^2\right]^{\frac{1}{2}}\right\}\right]\end{aligned} \tag{15}$$

Further, if the paraxial approximation:

$$\left[1-\left(2\pi\frac{f_n}{k_n}\right)^2\right]^{\frac{1}{2}}\simeq 1-2\left(\pi\frac{f_n}{k_n}\right)^2 \qquad (n=i,\ s) \tag{16}$$

is assumed with respect to the optical axis of the upconverter for the infrared and sum frequency wave, then

$$\underline{F}_s(f\ ;\ z_s)=-j\beta_s L\cdot\exp\{j2\pi^2\sigma_s f^2\}\cdot\underline{F}_{we}(f\ ;\ z_o)*[\underline{F}_i(f\ ;\ z_i)\exp\{j2\pi^2\sigma_i f^2\}] \tag{17}$$

In Eq. (17), the constant phase factor $\exp\{-jk_i z_{oi}-jk_s z_{so}\}$ that does not affect the images is omitted. Further,

$$\sigma_i\equiv\frac{z_{oi}}{k_i} \tag{18}$$

and

$$\sigma_s\equiv\frac{z_{so}}{k_s} \tag{19}$$

3.3. Case for a Gaussian beam pumping

From Eq. (17), the properties of the image upconverter are determined by the Fourier spectrum of the effective window function given by Eq. (11). In the case of the Gaussian beam pumping, the use of Eq. (9) gives

$$\underline{F}_{we}(f\ ;\ z_o)=\underline{F}_1(f\ ;\ z_o)*\underline{F}_2(f\ ;\ z_o)=\frac{w_{o1}w_{o2}}{w_1w_2}\frac{\pi}{\alpha}\exp\{-C(\rho_1-\rho_2)^2\}\cdot\exp\left[-\frac{\pi^2}{\alpha}\left\{(f-f_p)^2-\frac{j}{\pi}\mu\cdot(f-f_p)\right\}\right] \tag{20}$$

(See Appendix A.) Here,

$$f_p\equiv f_1+f_2 \tag{21}$$

$$\alpha\equiv\alpha_1+\alpha_2 \tag{22}$$

$$\mu\equiv 2(\alpha_1\rho_1+\alpha_2\rho_2) \tag{23}$$

and

$$C\equiv\frac{\alpha_1\alpha_2}{\alpha_1+\alpha_2} \tag{24}$$

The constant phase factor $\exp\{-j(k_1z_{o1}+k_2z_{o2}-\phi_1-\phi_2)\}$ is omitted since it does not affect the detected image.

In the limit of

$$\alpha\to 0 \tag{25}$$

Eq. (20) becomes

$$\underline{F}_{we}(f\ ;\ z_o)\propto\delta(f-f_p) \tag{26}$$

by the use of the Dirac delta function and corresponds to the plane wave pumping [7].

4. Phase-Matching Characteristics

4.1. Response for a plane-wave input

To study the phase-matching characteristics of the image upconverter, a plane wave expressed as

$$\underline{F}_i(f\ ;\ z_i)=\delta(f-f_i) \tag{27}$$

is assumed as the Fourier spectrum of the incident infrared wave. Here, the constant f_i is the spatial frequency of the infrared plane wave. If the sum frequency response is obtained by Eq. (17),

$$\underline{F}_s(f\ ;\ z_s)=-j\beta_s L\cdot\underline{F}_{we}(f-f_i\ ;\ z_o)\cdot\exp\{j2\pi^2(\sigma_s f^2+\sigma_i f_i^2)\} \tag{28}$$

Further, as the window function in the Gaussian beam pumping, Eq. (20) is substituted. Then,

$$\underline{F}_s(f\ ;\ z_s)=-j\beta_s L\frac{w_{o1}w_{o2}}{w_1w_2}\frac{\pi}{\alpha}\exp\{-C(\rho_1-\rho_2)^2\}\cdot\exp\left\{-\frac{\pi^2}{\alpha}\left(f'^2-\frac{j}{\pi}\mu\cdot f'\right)\right\}\cdot\exp\{j2\pi^2(\sigma_s f^2+\sigma_i f_i^2)\} \tag{29}$$

where

$$f'=f-f_i-f_p \tag{30}$$

In the plane-wave pumping, the sum frequency response for the plane-wave infrared input also becomes a plane wave [7]. On the other hand, Eq. (29) indicates that the response has a Fourier spectrum with a Gaussian distribution in the case of a Gaussian beam pumping.

4.2. Phase-matching characteristics

If the center frequency of the sum frequency Fourier spectrum is defined by the spatial frequency $(f_s)_{\max}$ at which the response is the maximum, then from Eq. (29)

$$|\underline{F}_s(f\ ;\ z_s)|\propto\exp\left[-\pi^2\frac{\alpha_r}{|\alpha|^2}\left\{\left(f'+\frac{1}{2\pi\alpha_r}(\alpha_r\mu_i-\alpha_i\mu_r)\right)^2-\frac{1}{4\pi^2\alpha_r^2}(\alpha_r\mu_i-\alpha_i\mu_r)^2\right\}\right] \tag{31}$$

$$(f_s)_{\max}=f_i+f_p-\frac{1}{2\pi\alpha_r}(\alpha_r\mu_i-\alpha_i\mu_r) \tag{32}$$

(See Appendix B.) Here, the real and imaginary parts of α and μ are

$$\left.\begin{aligned}\alpha &= \alpha_r + j\alpha_i \\ \mu &= \mu_r + j\mu_i\end{aligned}\right\} \tag{33}$$

If Eqs. (4), (22) and (23) are used, Eq. (23) becomes

$$(f_s)_{max} = f_i + f_p + \delta f_p \tag{34}$$

where

$$\delta f_p = \frac{1}{2\pi\alpha_r}\left(\frac{k_2}{w_1^2 R_2} - \frac{k_1}{w_2^2 R_1}\right)(\rho_1 - \rho_2) \tag{35}$$

Equation (34) is a representation of the phase matching in the parametric interaction in the spatial frequency domain.

In the case of a plane-wave pumping, the limits

$$\left.\begin{aligned}R_1, R_2 &\to \infty \\ w_1, w_2 &\to \infty\end{aligned}\right\} \tag{36}$$

are assumed. Then,

$$\delta f_p \to 0 \tag{37}$$

If Eq. (26) is used, the sum frequency response becomes a plane wave of a spatial frequency of f_s and

$$f_s = f_i + f_p \tag{38}$$

can be shown [7]. In this case, the subscript "max" in Eq. (34) is not used since only one spatial frequency component is contained in the response.

In the case of a Gaussian beam pumping, it is assumed for simplicity that

$$k_p = k_1 = k_2 \tag{39}$$

and

$$w = w_1 = w_2 \tag{40}$$

Then,

$$\delta f_p = \frac{k_p}{4\pi}\left(\frac{1}{R_2} - \frac{1}{R_1}\right)(\rho_1 - \rho_2) \tag{41}$$

Therefore, if

$$R_1 \neq R_2 \quad \text{and} \quad \rho_1 \neq \rho_2 \tag{42}$$

then

$$\delta f_p \neq 0 \tag{43}$$

holds. Since the radius of curvature R_m of the Gaussian beam depends on z_{om} (m = 1, 2), δf_p given by Eq. (41) is a function of the spatial coordinate ρ_m and z_{om}. Hence, if Eq. (42) holds, the phase-matching characteristics of the Gaussian beam-pumping system also depends on the spatial location of the beams. This fact is significantly different from the case of a plane-wave pumping in which the characteristics depend only on the spatial frequency of each pumping beam.

5. Image-Forming Properties

5.1. Optical field distribution of the sum frequency image

The optical field distribution of the sum frequency image response for an arbitrary infrared image input can be obtained by inverse Fourier transforming both sides of Eq. (17) as

$$\begin{aligned}E_s(\boldsymbol{\rho}\,;\,z_s) &= \frac{j\beta_s L}{4\pi^2\sigma_i\sigma_s}\iint d^2\boldsymbol{\rho}'\,d^2\boldsymbol{\rho}''\,E_{we}(\boldsymbol{\rho}''\,;\,z_o) \\ &\quad\cdot E_i(\boldsymbol{\rho}'\,;\,z_i)\exp\left\{\frac{1}{j2\sigma_i}(\boldsymbol{\rho}''-\boldsymbol{\rho}')^2\right\} \\ &\quad\cdot\exp\left\{\frac{1}{j2\sigma_s}(\boldsymbol{\rho}-\boldsymbol{\rho}'')^2\right\}\end{aligned} \tag{44}$$

where the function $E_{we}(\boldsymbol{\rho}\,;\,z_o)$ contained in the integrand is the inverse Fourier transform of $\underline{F}_{we}(\boldsymbol{f}\,;\,z_o)$. In the case of a Gaussian beam pumping, from Eq. (20)

$$\begin{aligned}E_{we}(\boldsymbol{\rho}\,;\,z_o) &= \frac{w_{o1}w_{o2}}{w_1 w_2}\exp\{-\alpha_1\rho_1^2 - \alpha_2\rho_2^2\} \\ &\quad\cdot\exp\{-\alpha\rho^2 + (\mu_r + j\mu_i')\cdot\boldsymbol{\rho}\}\end{aligned} \tag{45}$$

where

$$\mu_i' = \mu_i - 2\pi f_p \tag{46}$$

If Eq. (45) is substituted into Eq. (44),

$$\begin{aligned}E_s(\boldsymbol{\rho}\,;\,z_s) &= \frac{-j\beta_s L}{4\pi A\sigma_i\sigma_s}\frac{w_{o1}w_{o2}}{w_1 w_2}\exp\{-\alpha_1\rho_1^2 - \alpha_2\rho_2^2\} \\ &\quad\cdot\exp\left\{\frac{1}{j2\sigma_s}\rho^2 - \frac{\mu_r^2}{4A}\right\}\int d^2\boldsymbol{\rho}'E_i(\boldsymbol{\rho}'\,;\,z_i) \\ &\quad\cdot\exp\left\{\frac{1}{j2\sigma_i}\rho'^2 + \frac{\boldsymbol{\xi}'^2}{4A} - \frac{j}{2A}\mu_r\cdot\boldsymbol{\xi}'\right\}\end{aligned} \tag{47}$$

where

$$\boldsymbol{\xi}' \equiv \frac{\boldsymbol{\rho}'}{\sigma_i} + \frac{\boldsymbol{\rho}}{\sigma_s} + \mu_i' \tag{48}$$

and

$$A \equiv -\alpha + \frac{1}{j2}\left(\frac{1}{\sigma_i} + \frac{1}{\sigma_s}\right) \tag{49}$$

5.2. Imaging equation in the axial direction

Let us study first the imaging in the axial direction. In the limit of

$$A \to 0 \tag{50}$$

the Gaussian exponent factor contained in the right-hand side of Eq. (47) converges as

$$-\frac{1}{4\pi A}\exp\left\{\frac{\boldsymbol{\xi}'^2}{4A}\right\} \to \delta(\boldsymbol{\xi}') \tag{51}$$

Since $\delta(\xi')$ has a nonzero value only at $\xi' = 0$, the right-hand side of Eq. (47) can be integrated readily and

$$E_s(\boldsymbol{\rho}\,;\, z_s) \propto E_i\left(-\sigma_i\left(\frac{\boldsymbol{\rho}}{\sigma_s} + \boldsymbol{\mu}_i'\right)\,;\, z_i\right) \tag{52}$$

holds. In practice, the real part of A has a nonzero finite value from Eqs. (4), (22) and (49). This indicates the diffraction effect by the spot sizes of the Gaussian beams. On the other hand, the imaginary part of A can be made zero by adjusting the location of each image plane. If Eq. (50) is applied to the imaginary part of A, we obtain

$$\alpha_i + \frac{1}{2}\left(\frac{1}{\sigma_i} + \frac{1}{\sigma_s}\right) = 0 \tag{53}$$

This corresponds to the axial imaging equation in the geometric optics. If Eqs. (4), (18) and (19) are used, Eq. (53) is expressed as

$$\frac{k_i}{z_{oi}} + \frac{k_s}{z_{so}} + \frac{k_1}{R_1} + \frac{k_2}{R_2} = 0 \tag{54}$$

As a special case, in the limit of

$$R_1, R_2 \to \infty \tag{55}$$

Eq. (54) becomes

$$\frac{k_i}{z_{oi}} + \frac{k_s}{z_{so}} = 0 \tag{56}$$

This corresponds to the plane-wave pumping [7]. If the radii of curvature of the Gaussian beams are rewritten as

$$\begin{cases} R_1 \to z_{o1} \\ R_2 \to z_{o2} \end{cases} \tag{57}$$

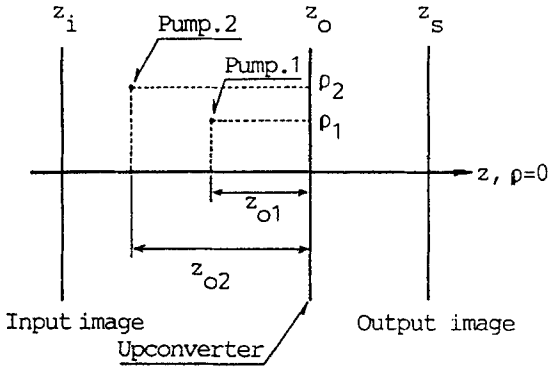

Fig. 5. Point source pumping.

then Eq. (54) coincides with the imaging equation of the point source pumping system in which the distances from the interaction plane are z_{o1} and z_{o2} as shown in Fig. 5 [9].

5.3. Imaging equation in the transverse direction

Next, the imaging in the transverse direction is studied. As the infrared input, the unit impulse located at the transverse coordinate $\rho = \rho_i$

$$E_i(\boldsymbol{\rho}\,;\, z_i) = \delta(\boldsymbol{\rho} - \boldsymbol{\rho}_i) \tag{58}$$

is assumed, which is substituted into Eq. (47). Then,

$$\begin{aligned} E_s(\boldsymbol{\rho}\,;\, z_s) &= \frac{j\beta_s L}{4\pi\alpha_r\sigma_i\sigma_s}\frac{w_{o1}w_{o2}}{w_1 w_2}\exp\{-C_r(\boldsymbol{\rho}_1 - \boldsymbol{\rho}_2)^2\} \\ &\cdot\exp\left\{\frac{1}{j2\sigma_s}\boldsymbol{\rho}^2 + \frac{1}{j2\sigma_i}\boldsymbol{\rho}_i^2\right\} \\ &\cdot\exp\left\{-\frac{\boldsymbol{\xi}^2}{4\alpha_r} + \frac{j}{2\alpha_r}\boldsymbol{\mu}_r\cdot\boldsymbol{\xi}\right\} \end{aligned} \tag{59}$$

where

$$\boldsymbol{\xi} \equiv \frac{\boldsymbol{\rho}_i}{\sigma_i} + \frac{\boldsymbol{\rho}}{\sigma_s} + \boldsymbol{\mu}_i' \tag{60}$$

and

$$C_r \equiv \frac{\alpha_{1r}\alpha_{2r}}{\alpha_{1r} + \alpha_{2r}} \tag{61}$$

and the imaging condition in Eq. (54) is assumed. Also, the real and imaginary parts of α_m (m = 1, 2) are expressed as α_{mr} and α_{mi}.

The phase factor $\exp\{-j\alpha_{1i}\rho_1^2 - j\alpha_{2i}\rho_2^2\}$ unaffecting the image is omitted.

Here, $\exp\{-C_r(\rho_1-\rho_2)^2\}$ indicates the relationship of the overlapping of the two pumping Gaussian beams on the interaction plane to the conversion efficiency ($\propto |E_s(\rho, z_s)|$) of the upconverter. The conversion efficiency becomes maximum when

$$\rho_1 = \rho_2 \tag{62}$$

namely, when the optical axes of the two beams coincide on the interaction plane. The sum frequency image has a Gaussian distribution and the transverse coordinate ρ_s of the center of the image is given by

$$\xi = 0 \tag{63}$$

This is written from Eqs. (4), (23), (46) and (60) as

$$\frac{k_i}{z_{oi}}\rho_i + \frac{k_s}{z_{so}}\rho_s + \frac{k_1}{R_1}\rho_1 + \frac{k_2}{R_2}\rho_2 = 2\pi f_p \tag{64}$$

which is the transverse imaging equation for the image upconverter. As a special case, when the radii of curvatures are infinite, Eq. (55) can be used and

$$\frac{k_i}{z_{oi}}\rho_i + \frac{k_s}{z_{so}}\rho_s = 2\pi f_p \tag{65}$$

This coincides with the imaging equation for the plane-wave pumping system [7]. Also, if Eq. (57) and $f_p = 0$ are assumed, Eq. (64) coincides with the imaging equation of the point source pumping system as shown in Fig. 5 [9].

6. Conclusions

The spatial frequency transfer properties were analyzed for an image converter with a thin nonlinear optical medium pumped by Gaussian beams. First, to study the effect of the location of the pumping beams on the image upconversion properties, the Fourier spectra of the Gaussian beams were derived with the parallel shift of the beam with respect to the upconversion system. For this Gaussian beam system with thin nonlinear medium, the spatial frequency transfer equation was applied, and the Fourier spectrum of the sum-frequency optical response for the plane-wave infrared input was derived.

The effects of various Gaussian beam parameters on the phase matching of the image upconverter were found. Especially, in comparison to the case of a plane-wave pumping in which the phase-matching characteristics depend only on the spatial frequency of the pumping beams, it was shown that the spatial orientations of the two beams and the spot sizes and the radii of curvatures on the interaction plane must be considered in the case of Gaussian beam pumping.

Second, by deriving the sum frequency optical field distribution for a unit impulse infrared wave, the imaging equations for the Gaussian beam-pumping system were derived. It was confirmed that the results agree under appropriate conditions with the imaging equations for a plane-wave pumping and for a point-source pumping so that the generality of the present imaging equations was confirmed. Further, the relationship between the overlap of the two pumping beams on the interaction plane and the conversion efficiency of the upconverter was investigated.

The results in this paper can be applied to the analysis of the spatial frequency transfer properties of a thick medium and of the Fourier mode optical system [14]. Also, they can be applied to the analysis of the resolution as well as the thickness aberation and the chromatic aberation in the paraxial ray.

Acknowledgement. The authors thank Dr. K. Sato, Lecturer of Faculty of Engineering, Hokkai-Gakuen University, for useful suggestions.

REFERENCES

1. I. Sakuraba. Properties of image upconverters and their applications. Japanese Journal of Optics, 11, 3, pp. 261-266 (June 1982).
2. A. Okamoto, K. Hisudome, T. Mishima, and I. Sakuraba. Signal-to-noise ratios of active image upconverters. Papers of Technical Group on Optics and Quantum Electronics, I.E.I.C.E., Japan, OQE85-144 (Feb. 1986).
3. K. S. Krishnan, J. S. Ostrem, E. A. Stappaerts. Infrared imaging using nonlinear optical upconversion. Opt. Eng., 17, 2, pp. 108-112 (March-April 1978).
4. A. Okamoto, T. Mishima, and I. Sakuraba. Image characteristics of an image upconverter using a thin medium. 1986 United Convention of Hokkaido Branches of Electricity Associated Institutes, 203 (1986).
5. A. Okamoto, K. Sato, T. Mishima, and I. Sakuraba. Fourier-transformed coupled wave-equation of two-photon-pumped image upconverter. I.E.I.C.E. Trans. (C), J71-C, 1, pp. 155-156 (Jan. 1988).
6. A. Okamoto, K. Sato, T. Mishima, and I. Sakuraba. Fourier optical analysis

of an image upconverter-plane wave pumping. I.E.I.C.E. Tech. Rept., EID87-16 (June 1987).
7. A. Okamoto, K. Sato, T. Mishima, and I. Sakuraba. Optical transfer properties of two-photon-pumped image upconverter--In the case of plane-wave pumping. I.E.I.C.E. Trans. (C), J71-C, 8, pp. 1164-1170 (Aug. 1988).
8. S. Sasaki, T. Mishima, and I. Sakuraba. Thickness aberations in two-photon-resonant image upconverters. I.E.C.E. Trans. (C), J63-C, 9, pp. 593-600 (Sept. 1980).
9. K. Sato and I. Sakuraba. Diffraction integral representation of two-photon-resonant image upconverter. I.E.C.E. Trans. (C), J67-C, 4, pp. 353-360 (Apr. 1984).
10. J. H. Newton and J. F. Young. Infrared image upconversion using two-photon-resonant optical four-wave mixing in alkali metal vapors. IEEE J. Quantum Electron., QE-16, 3, pp. 268-276 (March 1980).
11. I. Sakuraba. Laser Engineering. Morikita Publ. (1984).
12. J. W. Goodman. Introduction to Fourier Optics. McGraw-Hill, New York (1968).
13. D. M. Bloom, J. T. Yardley, J. F. Young, and S. E. Harris. Infrared upconversion with resonantly two-photon-pumped metal vapors. Appl. Phys. Lett., 24, 9, pp. 427-428 (1974).
14. R. E. Andrews. IR image parametric upconversion. IEEE J. Quantum Electron., QE-6, 1, pp. 68-80 (1970).

APPENDIX

A. Derivation of Eq. (20)

The inverse Fourier transform of Eq. (9) is

$$\begin{aligned} E_m(\boldsymbol{\rho}\,;z_o) &\equiv \int \underline{F}_m(\boldsymbol{f}\,;z_o)\exp\{-j2\pi \boldsymbol{f}\cdot\boldsymbol{\rho}\}d^2\boldsymbol{f} \\ &= \frac{w_{om}}{w_m}\exp\{-j(k_m z_{om}-\phi_m)-\alpha_m(\boldsymbol{\rho}-\boldsymbol{\rho}_m)^2 \\ &\quad -j2\pi \boldsymbol{f}_m\cdot\boldsymbol{\rho}\} \end{aligned} \tag{A1}$$

If the Fourier transform operator is $\mathcal{F}$, Eq. (20) can be obtained from

$$\begin{aligned} \underline{F}_{we}(\boldsymbol{f}\,;z_o) &= \underline{F}_1(\boldsymbol{f}\,;z_o) * \underline{F}_2(\boldsymbol{f}\,;z_o) \\ &= \mathcal{F}\{E_1(\boldsymbol{\rho}\,;z_o)E_2(\boldsymbol{\rho}\,;z_o)\} \end{aligned} \tag{A2}$$

B. Derivation of Eq. (31)

Let $\alpha = \alpha^{-1}$ and $\alpha = \alpha_r + j\alpha_i$. Then, for the exponential factor expressing the phase matching characteristics,

$$\begin{aligned} &\left|\exp\left\{-\frac{\pi^2}{\alpha}\left(\boldsymbol{f}'^2-\frac{j}{\pi}\boldsymbol{\mu}\cdot\boldsymbol{f}'\right)\right\}\right| \\ &= \exp\left\{-\pi^2\left(\alpha_r \boldsymbol{f}'^2+\frac{\alpha_r}{\pi}\boldsymbol{\mu}_i\cdot\boldsymbol{f}'+\frac{\alpha_i}{\pi}\boldsymbol{\mu}_r\cdot\boldsymbol{f}'\right)\right\} \\ &= \exp\left[-\pi^2\alpha_r\left\{\left(\boldsymbol{f}'+\frac{1}{2\pi\alpha_r}(\alpha_r\boldsymbol{\mu}_i+\alpha_i\boldsymbol{\mu}_r)\right)^2 \right.\right. \\ &\quad \left.\left. -\frac{(\alpha_r\boldsymbol{\mu}_i+\alpha_i\boldsymbol{\mu}_r)^2}{4\pi^2\alpha_r^2}\right\}\right] \end{aligned} \tag{A3}$$

By using $\alpha_r = \alpha_r/|\alpha|^2$ and $\alpha_i = -\alpha_i/|\alpha|^2$, Eq. (31) is obtained.

AUTHORS (from left to right)



Atsushi Okamoto graduated in 1985 from the Dept. Electronic Engineering, Hokkaido University, and obtained a Dr. of Eng. degree in 1990. Presently, he is a Lecturer at the same University. He has been engaged in research on nonlinear optical devices.

Teruhito Mishima graduated in 1969 from the Dept. Electronic Engineering, Hokkaido University, and obtained a Dr. of Eng. degree in 1974. In that year, he became a Lecturer at the same University. Since then he has been engaged in research on quantum electronics and optical devices. After serving as an Associate Professor, he was promoted to Professor. He is a member of the Optical Society of Japan; the Japan Society of Applied Physics Optical Research Group; and IEEE.

Ichiro Sakuraba graduated in 1949 from the Dept. Electrical Engineering, Hokkaido University. After working at Hokkaido Power, he obtained a Dr. of Eng. degree in 1959. After serving as an Associate Professor in the same University, he was on leave at the University of Michigan in 1963 and promoted to a Professor in 1965. In 1990, he became an Emeritus Professor and he is now a Professor of Electronics and Information Engineering, Hokkai-Gakuen University. He has been engaged in nonlinear optical devices. He is the author of Laser Engineering and Introduction to Optoelectronics. He is a member of IEEE.